



Changes in dissolved inorganic carbon in river water due to urbanization revealed by hydrochemistry and carbon isotope in the Pearl River Delta, China

Yingxue Xuan¹ · Yingjie Cao^{2,3} · Changyuan Tang^{1,2,3} · Miao Li⁴

Received: 20 December 2019 / Accepted: 16 March 2020 / Published online: 19 April 2020
© Springer-Verlag GmbH Germany, part of Springer Nature 2020

Abstract

Under natural conditions, the dissolved inorganic carbon (DIC) in river water is dominantly derived from carbonate or silicate dissolution by carbonic acid. However, sulfuric and nitric acids produced by human activities provide additional acidity for chemical weathering, which would affect the DIC flux and change its isotopic composition. To identify the natural and anthropogenic impacts on DIC, the major ion concentrations and stable carbon isotopes of the DIC ($\delta^{13}\text{C}$ -DIC) of river waters were measured in the Pearl River Delta (PRD) region, which is one of the most developed and populated areas in China. The mass balance calculations for DIC-apportionment showed that carbonate dissolution by carbonic acid was the dominant origin of DIC in the Beijiang (BJ) River (67%) and Xijiang (XJ) River (78%) and silicate dissolution by carbonic acid was the dominant origin of DIC in the Guangzhou (GZ) Channel (37%) and Dongjiang (DJ) River (50%), which was related to the lithology of the catchment. The contribution of carbonate dissolution by sulfuric and nitric acids, which represented the contribution of human activities to the total DIC concentrations in river water, showed high proportions in the GZ Channel and DJ River, with averages of 42% and 34%, respectively, which were associated with a high degree of urbanization. Evidence of hydrochemical parameters and $\delta^{13}\text{C}$ -DIC signatures indicated that human activities had impacts on the DIC pool. Carbonate dissolution by sulfuric and nitric acids caused by human activities changed DIC apportionments rather than the DIC flux, and this part of DIC would ultimately become a source of CO_2 to the atmosphere on the geological timescale and affects the CO_2 budget. An increase in nutrient concentration due to increased sewage discharge in the urbanized area could promote phytoplankton photosynthesis, which could change the DIC pool and increase the $\delta^{13}\text{C}$ -DIC value. This study quantitatively highlights the influence of human activities on DIC apportionment in river water, suggesting that anthropogenic impacts should be seriously considered when evaluating the evolution of DIC.

Keywords Dissolved inorganic carbon · Isotope · Urbanization · Hydrochemistry · Pearl River Delta

Responsible Editor: Zhihong Xu

✉ Changyuan Tang
tangchy2@mail.sysu.edu.cn; changyuan_tang@163.com

¹ School of Geography and Planning, Sun Yat-Sen University, Guangzhou, China

² School of Environmental Science and Engineering, Sun Yat-Sen University, No. 132, Wai Huan Dong road, University Town, Guangzhou 510006, People's Republic of China

³ GuangDong Provincial Key Laboratory of Environmental Pollution Control and Remediation Technology, Sun Yat-Sen University, Guangzhou, China

⁴ Development Research Center of the Ministry of Water Resources of P.R. China, Beijing, China

Introduction

Chemical weathering of rocks driven by carbonic acid that originates from CO_2 in the atmosphere or soil respiration under natural conditions is a fundamental geochemical process that links geochemical cycling of land to the atmosphere and ocean (Guo et al. 2015; Liu et al. 2018a), which regulates Earth's climate and can convert atmospheric/soil CO_2 into dissolved inorganic carbon (DIC) (Li et al. 2008; Murphy et al. 2016). This DIC is transported by rivers or groundwater and is thereafter precipitated in the ocean as carbonate minerals (Jiang 2013; Li et al. 2008). Carbonate and silicate weathering driven by carbonic acid are recognized as two typical categories

of chemical weathering. Carbonate dissolution driven by carbonic acid can cause the accumulation or depletion of CO_2 on short timescales, and the CO_2 consumption on the continents is balanced by the flux of CO_2 released into the atmosphere from the oceans by carbonate precipitation on the geological timescale (Berner and Kothavala 2001). The consumption of CO_2 during silicate dissolution driven by carbonic acid has been regarded as the net sink of CO_2 and regulates the global carbon cycle on the geological timescale (Hartmann et al. 2014; Lerman and Wu 2006). Although carbonate and silicate dissolution by carbonic acid are dominant weathering processes in a carbonate-silicate mixing ecosystem, other acids (such as sulfuric and nitric acids) of anthropogenic origins also provide the required acidity and become important chemical weathering agents (Ali and Atekwana 2011; Barnes and Raymond 2009; Cartwright 2010; Cuoco et al. 2017; Gandois et al. 2011; Raymond et al. 2008; Spence and Telmer 2005; Xia et al. 2017). In these cases, carbonate dissolution driven by sulfuric and nitric acids may result in increased DIC export in agricultural or urban areas (Jiang 2013) and become a source of CO_2 to the atmosphere on the geological timescale, which plays a crucial role in balancing the CO_2 budget (Li et al. 2008). Thus, under the influence of human activities, carbonate dissolution by the combination of carbonic, sulfuric, and nitric acids and silicate dissolution by carbonic acid control the net sink of atmospheric CO_2 , and it is essential to distinguish the contributions of these processes to DIC.

River have been recognized as an important pathway for the transport of DIC from land to the oceans. However, rivers are not passive transport agents of DIC produced by weathering processes to the oceans (Wachniew 2006) but are open systems linked to terrestrial ecosystems, groundwater, and the atmosphere (Michel 2003). Thus, biogeochemical processes occur are intertwined with physical processes in rivers, which results in a redistribution of carbon (Cuoco et al. 2017; Li et al. 2019; Yang et al. 2016). For example, DIC may be assimilated by primary producers and is incorporated into a complex aquatic food web, which involves the production and consumption of different forms of particulate or dissolved organic carbon (Gao and Wang 2015; Zavadlav et al. 2013). The DIC pool is also replenished by respiration from bacterial activities (Peter and James 2000) and photodissociation of auto- and allochthonous organic matter (Wachniew 2006). In addition, human activities such as the development of agriculture and industry and the increase in urbanization also affect riverine carbon cycling (Barnes and Raymond 2009). For example, photosynthesis and respiration processes are intensified by increases in nutrients and organic carbon caused by wastewaters and agricultural runoff inputs in rivers (Wachniew

2006). The export of DIC may increase due to urban and agricultural activities, which is related to enhanced CO_2 production by organic matter due to land disturbance activities (Barnes and Raymond 2009). Thus, it is important to identify the carbon cycles in rivers and understand how these biogeochemical processes, especially the processes affected by human perturbations, function in current weathering systems.

In aquatic ecosystems, the stable carbon isotopic composition of DIC ($\delta^{13}\text{C}$ -DIC) can reflect the integrated influence of biogeochemical processes in the water, including different sources, primary production, and carbonate chemistry (Niinikoski and Karhu 2017; Samanta et al. 2015; Schulte et al. 2011). Both the sources and internal biogeochemical processes of DIC can leave distinguishable traces in the stable carbon isotopic composition of DIC. For example, the $\delta^{13}\text{C}$ values for most carbonates range from -3 to $+2\text{‰}$ (Telmer and Veizer 1999). The $\delta^{13}\text{C}$ of atmospheric CO_2 ranges from -6 to -8‰ with an average of -7‰ (Levin et al. 1995), and the fractionation during dissolution of CO_2 ranges from $9.2 \pm 0.4\text{‰}$ at 0 °C to $6.8 \pm 0.4\text{‰}$ at 30 °C (Halas et al. 1997). The $\delta^{13}\text{C}$ of soil CO_2 , however, has a wide range ($-23 \sim -13\text{‰}$), which is inherited from decaying organic matter and depends largely on the photosynthetic pathway of vegetation (Vogel 1993). In addition, biogeochemical processes of DIC in the waters, such as photosynthesis and respiration, are also recorded in the $\delta^{13}\text{C}$ -DIC signatures (Dubois et al. 2010; Schulte et al. 2011). Thus, $\delta^{13}\text{C}$ -DIC is a valuable tracer in tracking sources of DIC and in understanding C cycling in aquatic ecosystems.

The Pearl River is the second largest river in China in terms of discharge volume and is characterized by a mixture of carbonate-silicate rocks in lithology. Over the past three decades, the Pearl River basin has undergone rapid urbanization and extensive agricultural development (Strokal et al. 2015; Zhang et al. 2007), resulting in a great influence of human activities on chemical weathering and the hydrochemical composition in the river water. The Pearl River Delta (PRD) region is located downstream of the Pearl River and is characterized by high levels of urbanization, dense populations, and extensive economic development (Hu and Li 2009; Lu et al. 2009). Thus, the hydrochemical composition of the PRD region can reflect both rock weathering processes and human activities affecting the water chemistry and biogeochemical processes of DIC. Therefore, in this study, the major physical-chemical parameters and the carbon isotope composition of river water in the PRD region were investigated to (1) identify the mechanisms controlling the major ion chemistry, (2) quantify the contributions of natural weathering processes and human activities to DIC, and (3) discuss the anthropogenic impacts on the DIC pool by $\delta^{13}\text{C}$ -DIC signatures.

Materials and methods

Study area

The PRD region is located in the subtropical area of South China and receives riverine inputs from the Pearl River, which consists of three major tributaries: the Dongjiang (DJ) River, Beijiang (BJ) River, and Xijiang (XJ) River (Fig. 1). The DJ River is characterized as the silicate-dominated area (Xie et al. 2013), the XJ River has carbonate as the main rock type (Gao and Wang 2015), and the BJ River is characterized as a typical mixed carbonate-silicate basin (Xuan et al. 2018). The PRD region has a monsoon climate with an average annual temperature between 20 and 25 °C and an average annual precipitation between 1600 and 2000 mm (Du et al. 2015; Zhou et al. 2011). The warm and wet climatic conditions make the PRD a hyperactive region in China. In this region, physical and biogeochemical processes show seasonal variations due to the regular variations between warm and humid monsoons in summer and cool and dry monsoons in winter (Ye et al. 2017; Ye et al. 2016). During the wet season (April to September), large nutrient and solute loadings are transported from the upper stream to the PRD region due to high precipitation and runoff (Ou et al. 2019; Yu et al. 2010, 2015). During the dry season (October to March), the water column is well mixed, resulting in intense physical processes due to the effect of reduced river discharge (Ye et al. 2017).

The Pearl River drains an area of 453,700 km². Over the past three decades, the Pearl River basin has experienced rapid urbanization and extensive agricultural development due to the Reform and Opening Up stage in China (Liu et al. 2018b; Xu et al. 2019). The dominant land uses in the upper drainage basin are forestry and agriculture, with the remainder used for urban areas or barren land (Xuan et al. 2018). The downstream area, which mainly consists of the PRD region, is dominated by agricultural land and urban and industrial use (Du et al. 2015). In addition, the PRD region is surrounded by a number of large metropolises, such as Guangzhou, Shenzhen, and Dongguan (Fig. 1). Therefore, in the PRD region, river water receives urban runoff, sewage inputs, and agricultural discharge from the upper stream and surrounding areas, which leads to a profound effect on the chemistry and biology of the river ecosystem.

Sample collection

Based on the precipitation and discharge, river water samples were collected in the PRD during the dry season in March 2018 and wet season in September 2018. The sampling

sites are shown in Fig. 1. The total number of river water samples was 116, including 58 samples in the wet season and 58 samples in the dry season. Specifically, in the PRD region, river water samples were collected from 14 sites in the Guangzhou (GZ) Channel, 15 sites in the DJ River, 13 sites in the BJ River, and 16 sites in the XJ River (Fig. 1).

At each sampling site, surface water samples (approximately 0.5 m below the surface) were collected with a water-sampling bottle (2 L). Water samples for $\delta^{13}\text{C}_{\text{DIC}}$ analysis were collected in 50 ml brown glass vials, and saturated HgCl_2 was added to prevent biological activity. Samples for major element analysis were filtered through a 0.45- μm glass fiber filter and stored in 100-ml tubes. All the water samples were stored below 4 °C until analysis.

Analysis method

Field parameters for river water samples including temperature (T), electric conductivity (EC), pH, and dissolved oxygen (DO) concentration were measured using a multi-parameter water quality meter (HACH-HQ40Q), and alkalinity of filtered water samples was measured by titration in situ. The nitrate (NO_3^-) concentrations were analyzed by continuous flow injection analyzer (AMS Alliance Integral Futura, Frepillon, France). The cations (Na^+ , K^+ , Ca^{2+} , Mg^{2+}) and anions (Cl^- , SO_4^{2-}) were analyzed by ion chromatography (ThermoFisher ICS-900) with limit of detection (L.O.D) of 0.01 mg/L. The ionic charge balance of the water samples was less than 5%. The dissolved SiO_2 was measured by molybdenum yellow method and was analyzed by ultraviolet spectrophotometer (Shimadzu UV-2600). Stable carbon isotope ratios of DIC ($\delta^{13}\text{C}_{\text{DIC}}$) were measured according to the method described by (Assayag et al. 2006). $\delta^{13}\text{C}_{\text{DIC}}$ analyses were performed on an elemental analysis-isotope ratios mass spectrometer (IRMS, Delta V Advantage) coupled with a GasBench II. All isotope analyses were conducted within 1 week after sampling. The analytical precision for $\delta^{13}\text{C}_{\text{DIC}}$ analysis was $\pm 0.06\%$. All laboratory analysis were made in the laboratory of School of Environmental Science and Engineering, Sun Yat-Sen University.

Data analysis

All statistical tests were conducted using SPSS version 22.0. Two-way ANOVA was used to test the seasonal and spatial differences in major ion concentrations and dissolved inorganic carbonate isotopes with significance at $p < 0.05$. DIC is defined as the sum of $[\text{CO}_2] + [\text{HCO}_3^-] + [\text{CO}_3^{2-}]$ in water samples, and the compositions of DIC were calculated by PHREEQC Interactive 3.1.4-8929. Principal component analysis (PCA) was

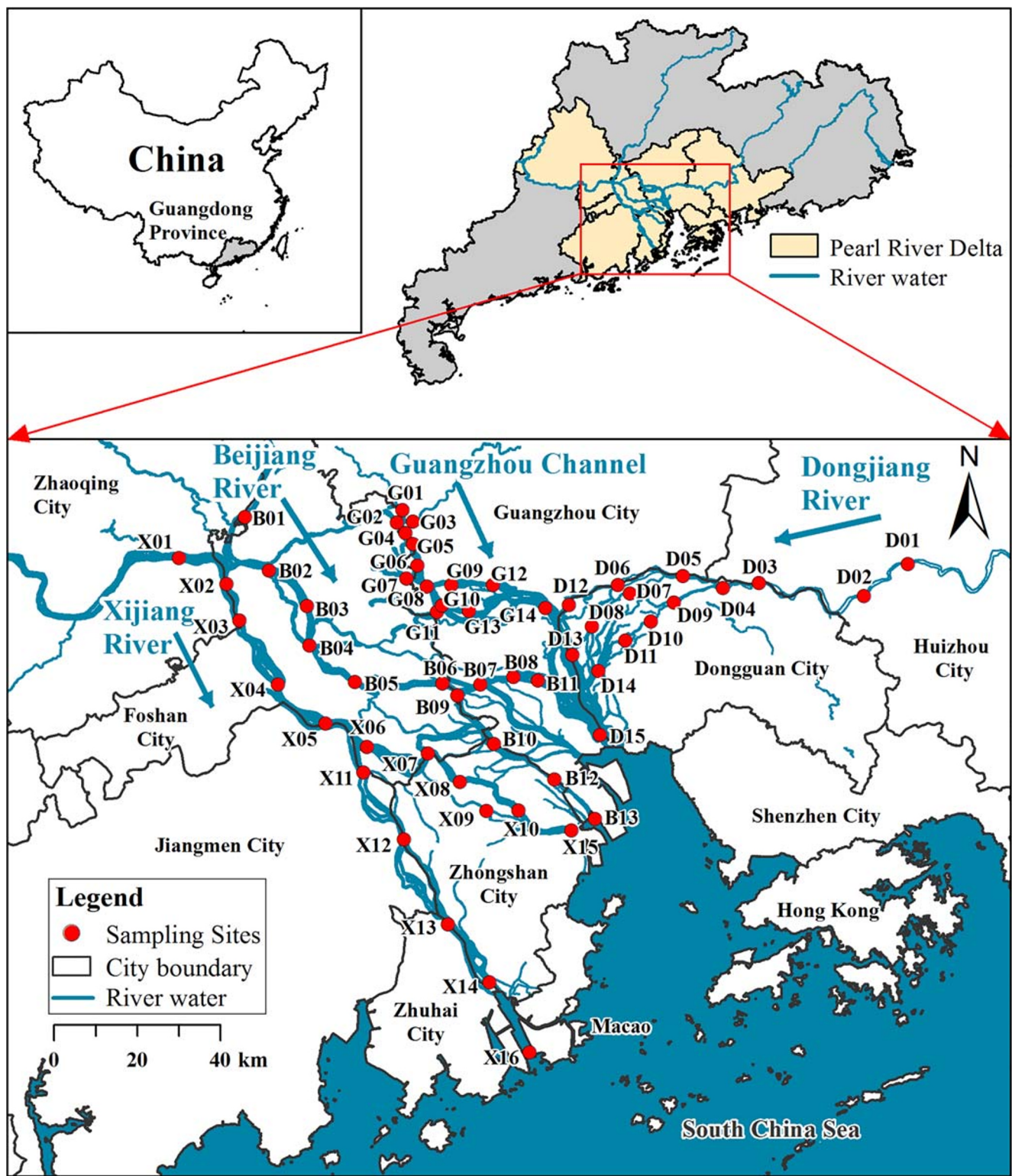


Fig. 1 Sampling sites in the Pearl River Delta

employed to unravel the underlying data set through the reduced new variables and analyzed the significant factors

affecting the characteristics of water chemistry. The map of sampling sites was generated by ArcGIS 10.2.

Results

Hydrochemical signatures of river water

The major physical-chemical parameters and the carbon isotope values of DIC ($\delta^{13}\text{C-DIC}$) in the river water samples are presented in Table 1. The surface water temperature was significantly higher in the wet season (mean \pm SD: 29.95 ± 0.95 °C) than in the dry season (20.36 ± 1.53 °C). The average of pH was 7.11 ± 0.48 in the wet season and 7.79 ± 0.42 in the dry season. The EC was higher in the dry season than in the wet season, ranging from 110 to 14,200 $\mu\text{s cm}^{-1}$. The EC increased from upstream to the lower estuary, with some slight fluctuations in the middle stream. The TDS of the river water samples varied from 32.66 to 1147.07 mg L^{-1} in the wet season and from 56.82 to 6146.28 mg L^{-1} in the dry season. The DIC which is defined as the sum of $[\text{CO}_2] + [\text{HCO}_3^-] + [\text{CO}_3^{2-}]$ can be calculated by using the alkalinity, water temperature, and pH. Based on calculation by PHREEQC, $[\text{CO}_2]$ and $[\text{CO}_3^{2-}]$ only account for less than 5% in most sampling sites; thus, the concentrations of HCO_3^- was used to represent the DIC in this study.

The major ion compositions of the river water samples in the PRD region are shown with Piper plot (Fig. 2). The river water samples were divided into three groups (I, II, and III) based on the major ion compositions (Fig. 2). Group I included most of the samples from the BJ River and the XJ River. In group I, Ca^{2+} was the dominant cation, accounting for approximately 69% of the total cations, followed by Mg^{2+} (15%), Na^+ (13%), and K^+ (3%); HCO_3^- was the dominant anion, which comprised 75% of the total anions, followed by SO_4^{2-} (13%), Cl^- (9%), and NO_3^- (3%), which suggested that the river water chemistry was controlled by chemical weathering rather than human activities. In the group II, river water samples mostly came from the GZ Channel and the DJ River, Ca^{2+} (49%) was also the predominant cation; however, the proportion of Na^+ was higher than that in group I, with an average of 34% of the total cations; HCO_3^- (49%) was also the predominant anion; however, the proportions of Cl^- , SO_4^{2-} , and NO_3^- were higher than those in group I, with averages of 23%, 21%, and 6% of the total anions, respectively, which indicated that the river water chemistry was affected by anthropogenic inputs. In group III, the samples were from the estuary region, which was characterized by high proportions of Na^+ (64%) and Cl^- (80%), indicating a mixing effect of river water and seawater.

$\delta^{13}\text{C}$ signatures of dissolved inorganic carbon

The $\delta^{13}\text{C}$ values of dissolved inorganic carbon in the rivers of the PRD region are given in Table 1. The $\delta^{13}\text{C-DIC}$ of river water samples exhibited a wide range, from -12.95 to -5.25‰ , with an average of $-9.15 \pm 1.60\text{‰}$. There were

significant seasonal variations in the $\delta^{13}\text{C-DIC}$ compositions of river waters ($p < 0.01$, by ANOVA), with lower values in the wet season ($-10.23 \pm 1.10\text{‰}$) and higher values in the dry season ($-8.02 \pm 1.18\text{‰}$). In addition, the spatial variations in the $\delta^{13}\text{C-DIC}$ were also significant ($p < 0.01$). During the wet season, the $\delta^{13}\text{C-DIC}$ values in the DJ River were the highest ($-9.20 \pm 1.03\text{‰}$), followed by the BJ River ($-9.98 \pm 0.97\text{‰}$) and XJ River ($-10.59 \pm 0.28\text{‰}$), and the $\delta^{13}\text{C-DIC}$ in the GZ Channel showed the lowest values with an average of $-11.18 \pm 0.94\text{‰}$. In contrast, during the dry season, the $\delta^{13}\text{C-DIC}$ values in the GZ Channel were the highest with an average of $-6.88 \pm 0.93\text{‰}$, followed by those in the DJ River ($-7.64 \pm 1.20\text{‰}$), BJ River ($-8.27 \pm 0.47\text{‰}$), and XJ River ($-9.13 \pm 0.66\text{‰}$). The $\delta^{13}\text{C-DIC}$ values measured in this study were similar to those from the Wuzhou and Makou stations in the Xijiang River ($-11.19\text{‰} \pm 1.18\text{‰}$) (Gao and Wang 2015), which are located in the upper stream of our study region. However, the $\delta^{13}\text{C-DIC}$ values in this study were significantly heavier than the $\delta^{13}\text{C-DIC}$ values measured in the southeast coastal river basin (-24.3 to -11‰) (Liu et al. 2018a) and Ottawa River and its tributaries (-17.4 to -7.3‰) (Telmer and Veizer 1999).

Discussion

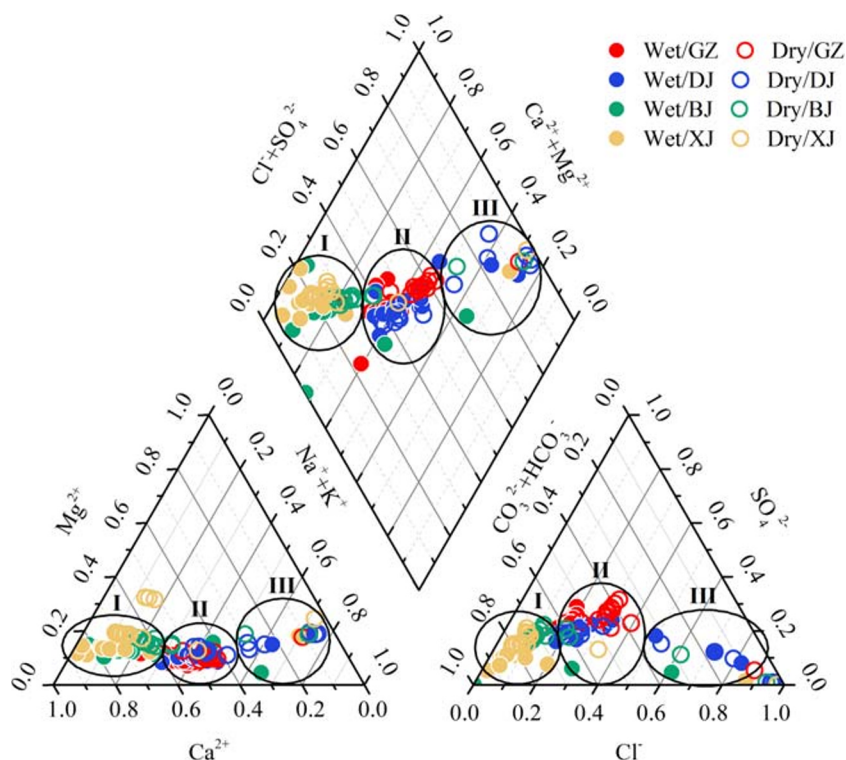
Mechanisms controlling the major ion chemistry

Principal component analysis (PCA) was used to study the factors controlling the chemical compositions, which is a multivariate technique that analyzes a data table representing the observations described by several intercorrelated quantitative dependent variables (Abdi and Williams 2010). The total dataset for the parameters of river water in the PRD was analyzed by PCA, and varimax rotation was used to reduce the number of variables to four principal components (PCs), which together explained 88.38% of the total variance in the data (Table 2). The first PC (PC1) explained approximately 38.18% of the total variations and had strong positive loadings on EC, Na^+ , K^+ , Mg^{2+} , and Cl^- , which was considered to represent the “salinity factor.” This factor indicated that salinity enhancement was caused by mineral dissolution and that salinity contributed to most of the TDS for water samples in the PRD region (Cao et al. 2016b; Yidana et al. 2008). The second PC (PC2) explained 20.03% of the total variance and presented high loadings for NO_3^- and SO_4^{2-} concentrations. This result was recognized as an “anthropogenic pollution” factor, which was identified in the areas with intensive urbanization development, industrialization, or agriculture due to domestic sewage discharge and agricultural activities (Cao et al. 2016a; Cuoco et al. 2017; Wen et al. 2018). As the PRD region is characterized by a high degree of urbanization (Liu et al. 2018b), the high concentrations of NO_3^- and SO_4^{2-}

Table 1 Minimum, maximum, and median values of major physical-chemical parameters, major ion concentrations, and $\delta^{13}\text{C-DIC}$ values of river waters. The total dissolved solid (TDS, mg L^{-1}) expressed as the sum of major inorganic species concentration ($\text{Na}^+ + \text{K}^+ + \text{Ca}^{2+} + \text{Mg}^{2+} + \text{HCO}_3^- + \text{Cl}^- + \text{SO}_4^{2-} + \text{NO}_3^- + \text{SiO}_2$). The results of seasonal and rivers variations were calculated by two-way ANOVA

Seasons	Rivers	Statistics	T (°C)	pH	EC (ms cm^{-1})	Na^+ (mg L^{-1})	K^+ (mg L^{-1})	Ca^{2+} (mg L^{-1})	Mg^{2+} (mg L^{-1})	Cl^- (mg L^{-1})	NO_3^- (mg L^{-1})	SO_4^{2-} (mg L^{-1})	SiO_2 (mg L^{-1})	HCO_3^- (mg L^{-1})	TDS (mg L^{-1})	$\delta^{13}\text{C-DIC}$ (‰)		
Wet season	Guangzhou Channel	Minimum	27.98	6.55	110.60	9.24	2.44	12.51	1.01	7.63	4.08	14.11	6.90	76.28	60.53	-12.95		
		Maximum	29.72	7.70	349.60	24.37	7.05	33.85	4.04	23.99	10.01	40.55	10.27	127.13	141.13	-9.69		
	Dongjiang River	Median	28.95	6.82	315.35	18.86	6.35	29.73	2.90	19.54	6.33	33.47	8.67	104.25	127.98	-10.83		
		Minimum	29.52	5.84	168.50	8.54	2.18	11.69	1.36	9.21	5.36	10.81	5.60	50.85	62.03	-10.51		
		Maximum	32.02	7.67	5214.10	281.90	12.60	37.46	37.50	578.07	12.36	76.35	10.57	116.96	1027.86	-6.55		
		Median	30.63	6.63	238.60	14.73	5.41	18.12	2.12	17.53	7.75	19.42	9.15	55.94	94.48	-9.21		
Dry season	Beijiang River	Minimum	28.72	7.00	225.40	0.08	0.68	9.58	1.05	0.10	0.04	4.89	6.77	91.53	33.51	-12.30		
		Maximum	32.12	8.34	1013.00	124.04	4.74	52.88	4.56	156.19	7.51	18.69	10.23	162.72	367.67	-7.95		
	Xijiang River	Median	30.46	7.45	252.90	6.07	2.43	30.59	3.53	6.19	3.57	14.34	8.61	116.96	75.41	-9.97		
		Minimum	28.91	7.19	270.30	0.02	0.79	24.16	1.99	1.58	0.11	6.42	6.94	122.04	46.52	-11.02		
		Maximum	31.08	7.75	4119.70	308.40	14.20	46.90	42.80	639.60	7.61	16.86	9.65	157.64	1077.07	-10.11		
		Median	29.59	7.34	279.55	4.40	2.07	41.26	4.38	5.98	3.61	15.00	7.63	147.47	85.69	-10.64		
Guangzhou Channel	Minimum	21.50	6.41	303.00	19.84	6.54	23.36	2.59	23.12	16.08	26.77	8.27	67.12	128.18	-8.19			
	Maximum	23.55	7.97	3080.00	431.68	23.10	60.52	57.25	862.00	32.00	73.23	9.88	140.35	1535.60	-5.40			
	Median	22.30	7.32	511.00	40.15	9.19	39.73	5.50	48.58	26.56	54.22	8.59	112.89	238.23	-7.14			
	Minimum	17.80	7.13	139.10	8.24	3.67	11.26	1.98	8.05	0.08	11.09	3.76	45.77	56.82	-9.31			
	Maximum	20.60	8.75	9850.00	1061.20	49.40	81.50	141.90	2407.97	13.05	48.62	10.89	128.14	3776.43	-5.25			
	Median	18.80	7.59	203.90	16.74	4.43	14.07	2.24	18.49	6.95	16.75	10.21	54.92	89.12	-7.84			
Beijiang River	Minimum	18.00	7.68	244.00	9.25	3.27	26.89	3.85	8.68	7.35	16.12	6.25	97.63	92.52	-8.83			
	Maximum	22.10	8.79	4230.00	600.40	29.20	62.40	82.90	1311.31	12.12	49.35	9.16	156.21	2122.30	-7.14			
	Median	20.20	8.06	275.00	10.75	3.81	31.97	4.80	10.90	8.67	24.79	7.85	115.94	103.37	-8.26			
	Minimum	18.90	7.66	312.00	5.72	2.21	37.96	6.85	5.97	0.76	22.44	6.08	131.19	101.68	-10.38			
	Maximum	22.00	8.25	14,200.00	2027.50	57.50	93.50	368.00	3584.35	10.25	34.68	9.14	167.81	6146.28	-8.09			
	Median	19.35	8.02	321.00	8.59	2.73	42.68	7.08	8.97	8.24	23.53	6.63	155.60	109.83	-9.10			
Statistics by ANOVA	Seasons	Minimum	$F = 3787.1$	$F = 112.3$	$F = 3.4$	$F = 4.5$	$F = 9.5$	$F = 11.6$	$F = 11.6$	$F = 5.0$	$F = 161.0$	$F = 33.6$	$F = 0.4$	$F = 0.8$	$F = 5.6$	$F = 199.3$	$p < 0.01$	
		Maximum	$p < 0.01$	$p < 0.01$	$p > 0.05$	$p < 0.05$	$p < 0.01$	$p < 0.01$	$p < 0.01$	$p < 0.05$	$p < 0.05$	$p < 0.01$	$p < 0.01$	$p > 0.05$	$p > 0.05$	$p < 0.05$	$p < 0.01$	
	Rivers	Minimum	$F = 6.6$	$F = 28.7$	$F = 1.1$	$F = 0.8$	$F = 3.1$	$F = 10.5$	$F = 10.5$	$F = 1.2$	$F = 87.7$	$F = 35.1$	$F = 10.7$	$F = 118.6$	$F = 0.9$	$F = 14.5$	$F = 14.5$	$p < 0.01$
		Maximum	$p < 0.01$	$p < 0.01$	$p > 0.05$	$p > 0.05$	$p < 0.01$	$p < 0.01$	$p < 0.01$	$p < 0.01$	$p > 0.05$	$p < 0.01$	$p < 0.01$	$p < 0.01$	$p < 0.01$	$p > 0.05$	$p < 0.01$	
	Season*Rivers	Minimum	$F = 46.4$	$F = 3.9$	$F = 0.4$	$F = 0.4$	$F = 0.2$	$F = 0.2$	$F = 0.2$	$F = 0.7$	$F = 75.5$	$F = 9.9$	$F = 4.0$	$F = 0.6$	$F = 0.5$	$F = 18.3$	$F = 18.3$	$p < 0.01$
		Maximum	$p < 0.01$	$p < 0.05$	$p > 0.05$	$p > 0.05$	$p > 0.05$	$p > 0.05$	$p > 0.05$	$p > 0.05$	$p > 0.05$	$p < 0.01$	$p < 0.01$	$p < 0.01$	$p > 0.05$	$p > 0.05$	$p < 0.01$	

Fig. 2 Piper diagram of river water during the wet season and dry season in the Pearl River Delta



come from domestic sewage and atmospheric deposition. The third component (PC3) explained 17.66% of the total variance and was considered a “rock weathering factor” because of the high contributions of Ca^{2+} , HCO_3^- , and SiO_2 . The fourth component (PC4) explained 12.49% of the total variance

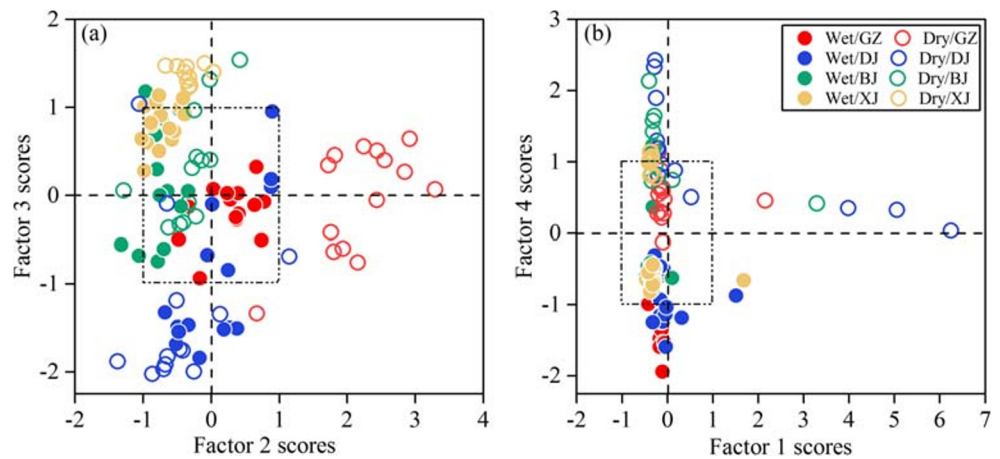
and had strong positive loadings on pH and $\delta^{13}\text{C-DIC}$, and the negative pole had a strong loading on temperature. This factor was defined as the “DIC source factor,” which reflected that the sources and transformations of DIC influenced the characteristics of hydrochemistry. In addition, the

Table 2 Rotated component matrix of principle component analysis for chemical parameters of river water in the Pearl River Delta

Parameters	PC1	PC2	PC3	PC4
Temperature	-0.161	-0.169	-0.012	-0.895
pH	-0.093	-0.270	0.325	0.811
EC	0.937	-0.016	0.138	0.006
DO	-0.066	-0.747	0.336	0.438
Na^+	0.995	-0.004	0.055	0.033
K^+	0.960	0.223	-0.064	0.037
Ca^{2+}	0.529	0.190	0.704	0.089
Mg^{2+}	0.987	-0.038	0.113	0.071
Cl^-	0.995	-0.029	0.054	0.035
NO_3^-	-0.099	0.902	-0.009	0.266
SO_4^{2-}	0.112	0.899	0.159	0.087
SiO_2	-0.096	0.043	-0.809	-0.030
HCO_3^-	-0.050	-0.060	0.947	0.018
$\delta^{13}\text{C-DIC}$	0.094	0.440	-0.280	0.729
Eigenvalue	3.819	2.003	1.766	1.249
% of variance	38.19	20.03	17.66	12.49
% of cumulative	38.19	58.22	75.89	88.38

The italics values indicate absolute component loadings higher than 0.5, which are considered significant contributors to the variance in the hydrochemistry

Fig. 3 Factor scores between factor 2 and factor 3 (a), and factor 1 and factor 4 (b) were calculated by SPSS 22.0 version for the parameters of river water in the Pearl River Delta. The dot line box shows the range of factor scores between -1 and +1



relationships between $\delta^{13}\text{C-DIC}$ and pH or temperature primarily reflected a strong dependence of $\delta^{13}\text{C-DIC}$ on pH and temperature values. First, the distribution of DIC species is set by pH; additions and withdrawals of CO_2 result in the decrease and increase in pH of river water, respectively, due to changes in the carbonate system equilibria; for example, dissolution of carbonates generally increases pH and $\delta^{13}\text{C-DIC}$ (Clark and Fritz 2013). Second, the changes in the $\delta^{13}\text{C-DIC}$ were also caused by photosynthetic assimilation, which was affected by temperature. Additions of the respired CO_2 decreased $\delta^{13}\text{C-DIC}$, while withdrawals of CO_2 via photosynthetic assimilation increased $\delta^{13}\text{C-DIC}$ (Wachniew 2006). Overall, in the PRD region, salinity, anthropogenic pollution, and rock weathering were treated as major factors controlling hydrochemistry, DIC was the major product of chemical weathering, and $\delta^{13}\text{C-DIC}$ could reflect biogeochemical processes and record the influences of those major factors on hydrochemistry. The mechanisms are discussed below.

Natural and anthropogenic factors

The factor scores were employed to quantify the differences in hydrochemistry on river water among different rivers and between different seasons in the PRD region (Fig. 3). As discussed above, factor 2 and factor 3 are represented as “anthropogenic factor” and “rock weathering factor or natural factor,” respectively. These two factors were treated as two major reasons resulting in spatial variation in hydrochemistry because the samples from different rivers were well separated by the scores of factor 2 and factor 3 (Fig. 3a). In Fig. 3a, most of samples from the BJ River and XJ River were located in the left quadrant with factor 2 scores ≤ 0 , and samples from the GZ Channel were located in the right quadrant with factor 2 scores ≥ 0 . This result implied that the influence of anthropogenic activities was higher in the GZ Channel and was lower in the BJ River and XJ River. Specifically, in the GZ Channel during the dry season, samples were “extremely affected” by anthropogenic activities with factor 2 scores higher than +1

(Fig. 3a). This finding suggested that the influence of anthropogenic factors was more effective in the dry season than in the wet season, which was related to the dilution of major ion concentrations by increased discharge in the wet season (Zeng et al. 2016). Figure 3a also shows that all of the samples from the XJ River were located in the upper quadrant with factor 3 scores ≥ 0 and most of the samples from the DJ River were located in the lower quadrant with factor 3 scores ≤ 0 , while samples from the GZ Channel and BJ River were not well separated by factor 3. These results indicated that (1) rock weathering had a great influence on river water in the XJ River and less influence on the river water in the DJ River and (2) the hydrochemistry in the GZ Channel and BJ River was controlled by mixing processes including rock weathering, anthropogenic activities, and others, such as biological sources (Cuoco et al. 2017; Ding et al. 2017).

Seasonal and spatial patterns of the $\delta^{13}\text{C-DIC}$ signature

As discussed above, factor 1 was recognized as the “salinity factor” and factor 4 was treated as the “DIC source factor”. The PRD region is characterized by a large deltaic and coastal system, and thus, samples characterized by high Na^+ and Cl^- concentrations were from the estuary region. Figure 3b shows that some of the samples were located in the right quadrant with factor 1 scores ≥ 0 , which suggested that the hydrochemistry of these samples was mainly affected by salinity and that these samples came from the estuary region. In addition, the samples from the wet season and the dry season were well separated by factor 4, showing factor 4 scores ≥ 0 for the dry season and factor 4 scores ≤ 0 for the wet season. This result suggested that DIC sources or relative biogeochemical processes of DIC exhibited significant seasonal variations in the PRD region because the $\delta^{13}\text{C-DIC}$ values were determined by contributions of different DIC sources with distinct isotopic compositions and fractionation effects during biogeochemical processes (Gao and Wang 2015; Li et al. 2019; Zavadlav et al. 2013). More detailed sources and

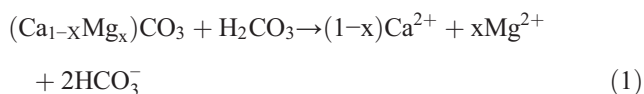
transformations of DIC are discussed in “Anthropogenic impacts on DIC.”

Anthropogenic impacts on DIC

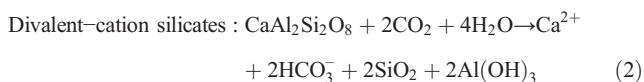
As discussed above, anthropogenic factors were one of the most important factors affecting the hydrochemistry of river water, and the effect of human activities on DIC exhibited significant spatial variations in the PRD region. Generally, under natural conditions, the DIC in river water is dominantly derived from carbonate and silicate dissolution by carbonic acid (Eqs. (1)–(3)); however, increases in human activities affect the DIC flux; for example, sulfuric and nitric acids contribute to carbonate dissolution (Eqs. (4) and (5)) and increase the DIC flux (Ali and Atekwana 2011; Barnes and Raymond 2009; Gandois et al. 2011). Carbonate dissolution and silicate dissolution under natural conditions and anthropogenic impact can be expressed as follows:

(a) Natural conditions:

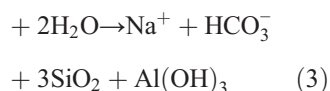
Weathering of carbonate minerals by H_2CO_3 :



Weathering of silicate minerals by H_2CO_3 :

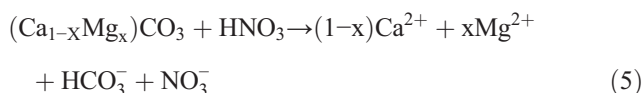
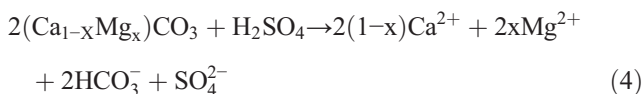


Monovalent-cation silicates : $NaAlSi_3O_8 + CO_2$

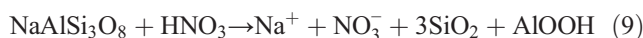
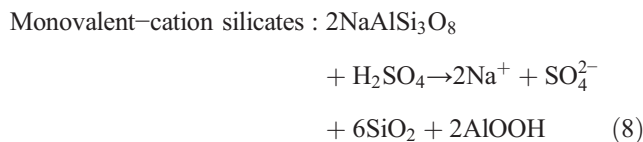
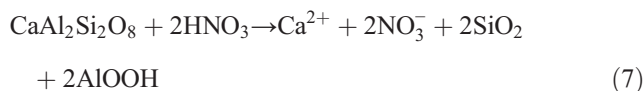
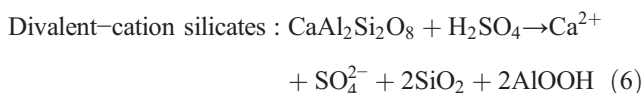


(b) Anthropogenic impact:

Weathering of carbonate minerals by H_2SO_4 and HNO_3 :

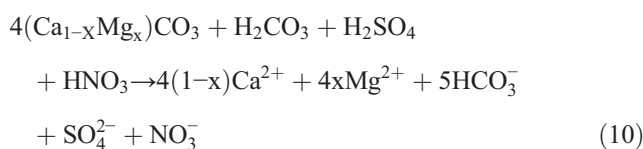


Weathering of silicate minerals by H_2SO_4 and HNO_3 :



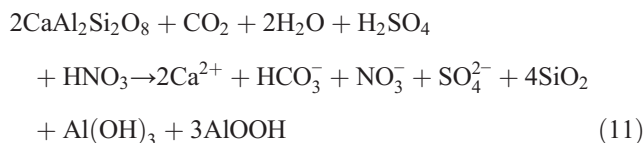
(c) Nature condition and anthropogenic impacts:

Weathering of carbonate minerals by H_2CO_3 , H_2SO_4 , and HNO_3 :

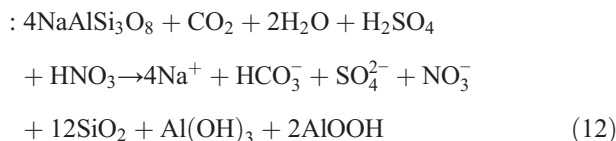


Weathering of silicate minerals by H_2CO_3 , H_2SO_4 , and HNO_3 :

Divalent-cation silicates:



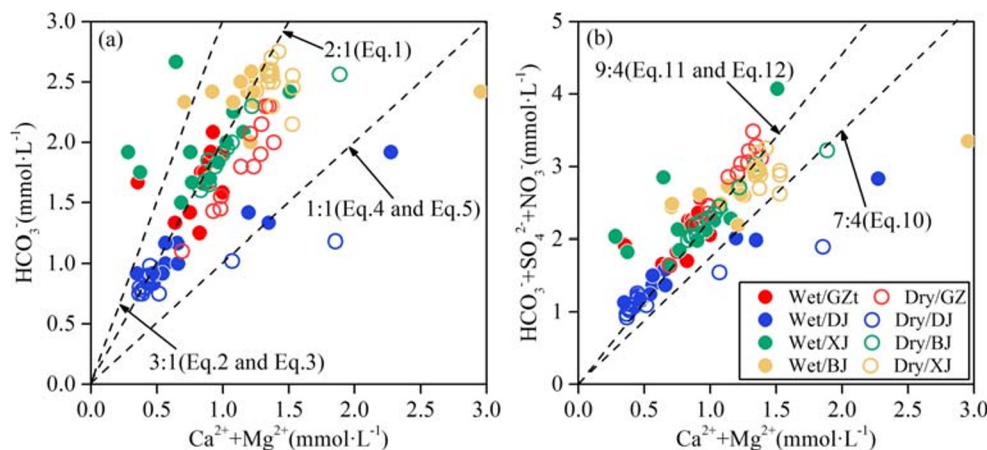
Monovalent-cation silicates



Contribution of human activities to DIC

In this study, the molar ratios between HCO_3^- and $(Ca^{2+} + Mg^{2+})$ of river water averaged 2.17 in the wet season (Fig. 4a), which was close to the expected molar ratios of HCO_3^- and $(Ca^{2+} + Mg^{2+})$ in carbonate dissolution by carbonic acid, according to Eq. (1). This result indicated that weathering of carbonate minerals by carbonic acids might be the dominant source of DIC, and rock weathering by other acids caused by human activities was not obvious in the wet season. The average molar ratio between HCO_3^- and $(Ca^{2+} + Mg^{2+})$ in river water during the dry season was 1.60, and those from the GZ Channel and DJ River were 1.50 and 1.40, respectively (Fig. 4a). According to Eqs. (4) and (5), the molar ratio between HCO_3^- and $(Ca^{2+} + Mg^{2+})$ is expected to be 1 when carbonate

Fig. 4 The relationships between **a** HCO_3^- and $(\text{Ca}^{2+} + \text{Mg}^{2+})$ and **b** $(\text{HCO}_3^- + \text{SO}_4^{2-} + \text{NO}_3^-)$ and $(\text{Ca}^{2+} + \text{Mg}^{2+})$ of river water in the Pearl River Delta



dissolution is controlled by sulfuric or nitric acid (Fig. 4a). The lower molar ratio between HCO_3^- and $(\text{Ca}^{2+} + \text{Mg}^{2+})$ in the dry season suggested that rock weathering by carbonic acids could not be a unique weathering agent and sulfuric or nitric acid caused by human activities played an important role in rock weathering during this period, especially in the GZ Channel and DJ River, which was characterized by a high degree of urbanization (Du et al. 2015).

In this case, the carbonate and silicate weathering by carbonic, sulfuric, and nitric acids were considered in this study. If the contributions of carbonic, sulfuric, and nitric acids to carbonate or silicate dissolution are in equimolar amounts, carbonate and silicate dissolution can be expressed as Eqs. (10), (11), and (12), and the molar ratio between $(\text{HCO}_3^- + \text{SO}_4^{2-} + \text{NO}_3^-)$ and $(\text{Ca}^{2+} + \text{Mg}^{2+})$ should be 7/4 (1.75) in carbonate dissolution and 9/4 (2.25) in the silicate dissolution (Fig. 4b). In the PRD region, the molar ratio between $(\text{HCO}_3^- + \text{SO}_4^{2-} + \text{NO}_3^-)$ and $(\text{Ca}^{2+} + \text{Mg}^{2+})$ in the river water varied from 1.24 to 5.40 in the wet season and from 1.44 to 2.81 in the dry season, indicating that mixed rock weathering including carbonate dissolution and silicate dissolution in the river water was controlled by carbonic, sulfuric, and nitric acids (Jiang 2013).

We assumed that f_1 , f_2 , and f_3 were the proportions of silicate dissolution contributed by carbonic acid, carbonate dissolution contributed by carbonic acid, and carbonate dissolution contributed by sulfuric and nitric acids to DIC, respectively. According to Eqs. (1)–(12), the contributions of silicate dissolution by carbonic acid (f_1) and carbonate dissolution by carbonic acid (f_2) could represent natural processes contributing to DIC, and the contributions of human activities to the DIC in river water were only through carbonate dissolution by sulfuric or nitric acids (f_3). The results of f_1 , f_2 , and f_3 can be calculated by the following steps.

First, the amounts of HCO_3^- derived from silicate dissolution and carbonate dissolution were calculated. In this study, precipitation inputs and evaporate weathering were

not carried out due to their minor influences on water chemistry in the river water in the PRD region (Zhang et al. 2007). The $\text{Ca}^{2+}/\text{Na}^+$ ratio of 0.4 and $\text{Mg}^{2+}/\text{Na}^+$ ratio of 0.2 for the silicate end-member in the Pearl River (Zhang et al. 2007) were used to calculate the contributions of Ca^{2+} and Mg^{2+} from silicate weathering, and then residual Ca^{2+} and Mg^{2+} were attributed to carbonate weathering. Thus, the concentrations of HCO_3^- derived from silicate dissolution and carbonate dissolution can be calculated by the following equations:

$$[\text{Cl}^-]_{\text{river}} = [\text{Cl}^-]_{\text{sea-salt}} = [\text{Na}^+]_{\text{sea-salt}} \tag{13}$$

$$[\text{K}^+]_{\text{river}} = [\text{K}^+]_{\text{silicate}} \tag{14}$$

$$[\text{Na}^+]_{\text{river}} = [\text{Na}^+]_{\text{sea-salt}} + [\text{Na}^+]_{\text{silicate}} \tag{15}$$

$$[\text{Ca}^{2+}]_{\text{river}} = [\text{Ca}^{2+}]_{\text{silicate}} + [\text{Ca}^{2+}]_{\text{carbonate}} \tag{16}$$

$$[\text{Mg}^{2+}]_{\text{river}} = [\text{Mg}^{2+}]_{\text{silicate}} + [\text{Mg}^{2+}]_{\text{carbonate}} \tag{17}$$

$$[\text{HCO}_3^-]_{\text{silicate}} = [\text{K}^+]_{\text{silicate}} + [\text{Na}^+]_{\text{silicate}} + 2[\text{Mg}^{2+}]_{\text{silicate}} + 2[\text{Ca}^{2+}]_{\text{silicate}} \tag{18}$$

$$[\text{HCO}_3^-]_{\text{carbonate}} = [\text{HCO}_3^-]_{\text{river}} - [\text{HCO}_3^-]_{\text{silicate}} \tag{19}$$

Second, the amounts of HCO_3^- derived from carbonate dissolution by carbonic acid were discriminated. According to Eqs. (1), (4), and (5), the results can be calculated by the following equation:

$$[\text{HCO}_3^-]_{\text{carbonate dissolution by carbonic acid}} = \left([\text{HCO}_3^-]_{\text{carbonate}} - [\text{Ca}^{2+} + \text{Mg}^{2+}]_{\text{carbonate}} \right) \times 2 \tag{20}$$

Third, the amounts of HCO_3^- derived from carbonate dissolution by sulfuric and nitric acids were discriminated as followed:

$$\begin{aligned}
 & [\text{HCO}_3^-]_{\text{carbonate dissolution by sulfuric and nitric acids}} \\
 &= [\text{HCO}_3^-]_{\text{carbonate}} - [\text{HCO}_3^-]_{\text{carbonate dissolution by carbonic acid}}
 \end{aligned}
 \quad (21)$$

Finally, the results of f_1 , f_2 and f_3 can be calculated as follows:

$$f_1 = [\text{HCO}_3^-]_{\text{silicate}} / [\text{HCO}_3^-]_{\text{river}} \times 100\% \quad (22)$$

$$\begin{aligned}
 f_2 &= [\text{HCO}_3^-]_{\text{carbonate dissolution by carbonic acid}} / [\text{HCO}_3^-]_{\text{river}} \\
 &\times 100\%
 \end{aligned}
 \quad (23)$$

$$f_3 = [\text{HCO}_3^-]_{\text{carbonate dissolution by sulfuric and nitric acids}} / [\text{HCO}_3^-]_{\text{river}} \times 100\% \quad (24)$$

The calculated results are presented in Fig. 5, and the proportions of different weathering processes contributing to the DIC showed significant spatial variations in the PRD region. The contributions of carbonate dissolution by carbonic acid to the total concentrations of DIC in river water were high in the BJ River and XJ River, averaging 67% and 78%, respectively. This result was related to the larger area ratios of carbonate rock outcrops in the BJ River (Xuan et al. 2018) and XJ River (Gao et al. 2009). The contributions of silicate dissolution by carbonic acid to the total concentrations of DIC in river water were high in the GZ Channel and DJ River, averaging 37% and 50%, respectively, which was associated with a larger proportion of silicate outcrops (Xie chenji et al. 2013). In addition, carbonate dissolution by sulfuric and nitric acids, which represented human activities contributing to DIC, showed high proportions in the GZ Channel and DJ River, with averages of 42% and 34%, respectively. As shown in

Fig. 5, the GZ Channel and the DJ River flow through the cities of Guangzhou and Dongguan, which are the metropolitan areas with high percentages of urbanized land, resulting in strong influences of human activities on water chemistry. Therefore, lithology (i.e., the nature of the rock) was the most important factor controlling the compositions of water chemistry; however, rock weathering was not controlled by only natural processes, and the influences of human activities on rock dissolution processes cannot be ignored, especially in highly urbanized areas.

$\delta^{13}\text{C}$ -DIC fingerprint of anthropogenic impacts on DIC

Mixing effect of different DIC sources The $\delta^{13}\text{C}$ -DIC composition of river water can reflect the contributions of DIC from different sources (Brunet et al. 2005; Spence and Telmer 2005). Here, the $\delta^{13}\text{C}$ -DIC signatures were used to validate the mass balance results. In this study, the contribution of atmospheric CO_2 to the DIC was minor due to the high partial pressure of CO_2 in river water (Gao and Wang 2015). Thus, the DIC mainly comes from two primary sources, soil CO_2 and carbonate bedrock. Soil CO_2 is a product of the decomposition of organic matter during periods of high biological activity and root respiration (Calmels et al. 2014; Rasse et al. 2001). Depending on the pH, the equilibrium dissolution of soil CO_2 into groundwater or river water resulted in the average $\delta^{13}\text{C}$ -DIC of -17‰ (Fig. 6) (Telmer and Veizer 1999). Most carbonate rocks, which originate in the oceans, result in marine $\delta^{13}\text{C}$, which has remained close to 0‰ since the end of the Proterozoic (Veizer et al. 1999). However, the $\delta^{13}\text{C}$ of marine carbonate rocks of Paleozoic to Tertiary age have an average of 0.5‰ (Faure 1977). In addition, the $\delta^{13}\text{C}$ of DIC

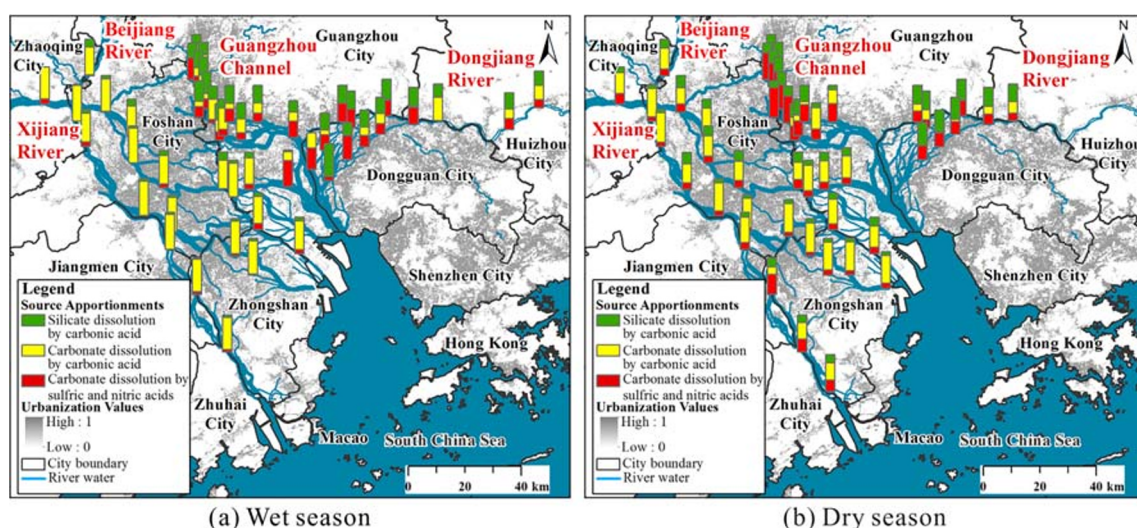


Fig. 5 Spatial distribution of contributed proportions of silicate dissolution by carbonic acid, carbonate dissolution by carbonic acid, and carbonate dissolution by sulfuric and nitric acids to DIC in the river

water during the wet season (a) and the dry season (b), together with the extent of urban land in the Pearl River Delta. Data of urban land was referenced from (Liu et al. 2018b)

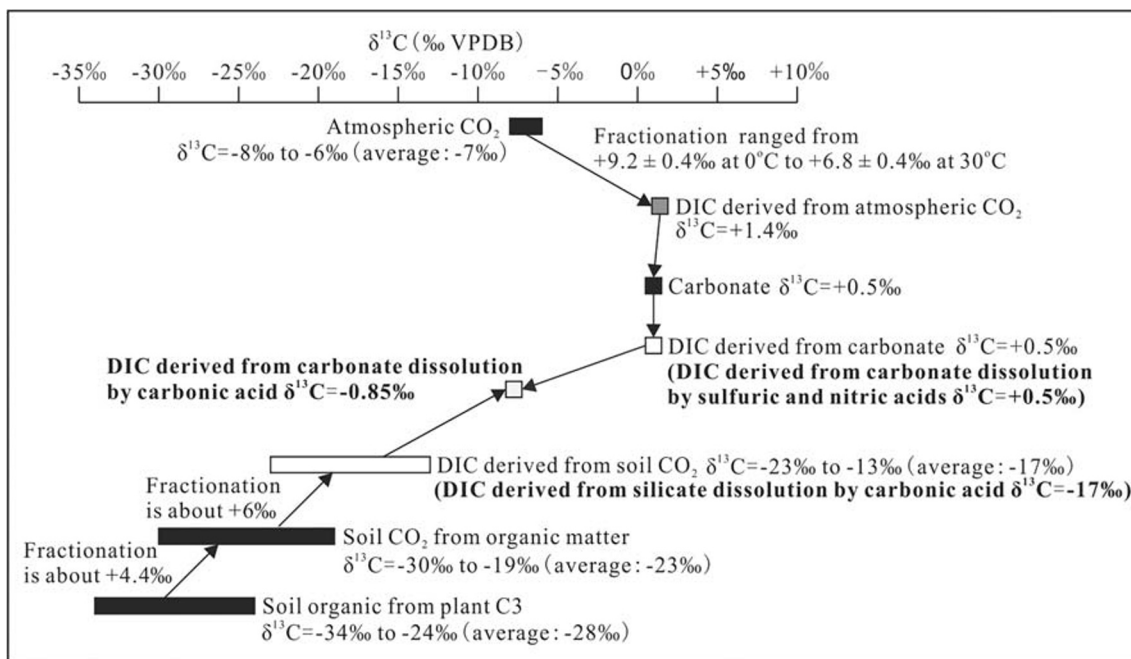


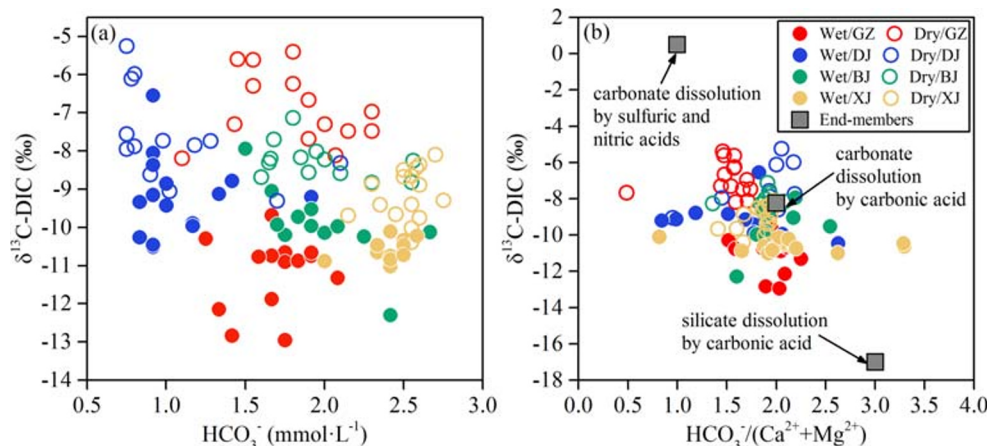
Fig. 6 Carbon isotopic signatures of various components of the carbon cycle in the river water system. White rectangles indicated the $\delta^{13}\text{C}$ -DIC of end-members used in this study. Modified from (Schulte et al. 2011)

could be affected by carbonate mineral precipitation (fractionation factor is approximately 1‰) (Zhang et al. 1995). Thus, to remain conservative, the DIC from carbonate dissolution had a $\delta^{13}\text{C}$ of 0.5‰ in this study (Fig. 6). Using the $\delta^{13}\text{C}$ -DIC values of primary sources and the stoichiometry of dissolution (Eqs. (1)–(12)), the $\delta^{13}\text{C}$ -DIC values of end-members for this study were defined as follows: (1) silicate dissolution by carbonic acid involved only carbon from soil CO_2 , producing the end-member of $\delta^{13}\text{C}$ -DIC = -17‰; (2) dissolution of 1 mole of calcium or magnesium carbonate ($\delta^{13}\text{C} = 0.5‰$) by carbonic acid involved 1 mole of dissolved soil CO_2 ($\delta^{13}\text{C} = -17‰$), producing an end-member of $\delta^{13}\text{C}$ -DIC = -8.25‰; (3) dissolution of carbonate by sulfuric and nitric acids involved only

carbon in calcium or magnesium carbonate, resulting in a $\delta^{13}\text{C}$ -DIC = +0.5‰ (Fig. 6).

The relationships between the $\delta^{13}\text{C}$ -DIC and major element ratios are presented in Fig. 7. As discussed in “Contribution of human activities to DIC,” the proportion of carbonate dissolution by sulfuric and nitric acids contributed to the DIC was high in the GZ Channel and DJ River; however, the DIC concentration was not higher than that in the BJ River and XJ River (Fig. 7a). This result suggested that although the contribution of carbonate dissolution by sulfuric and nitric acids to DIC increased, the export of DIC would not increase due to increases in sulfur and nitric acids by human activities. Thus, human activities changed only the

Fig. 7 The relationships between **a** $\delta^{13}\text{C}$ -DIC and HCO_3^- concentrations and **b** $\delta^{13}\text{C}$ -DIC and $\text{HCO}_3^-/(\text{Ca}^{2+}+\text{Mg}^{2+})$ ratios of river water in the Pearl River Delta



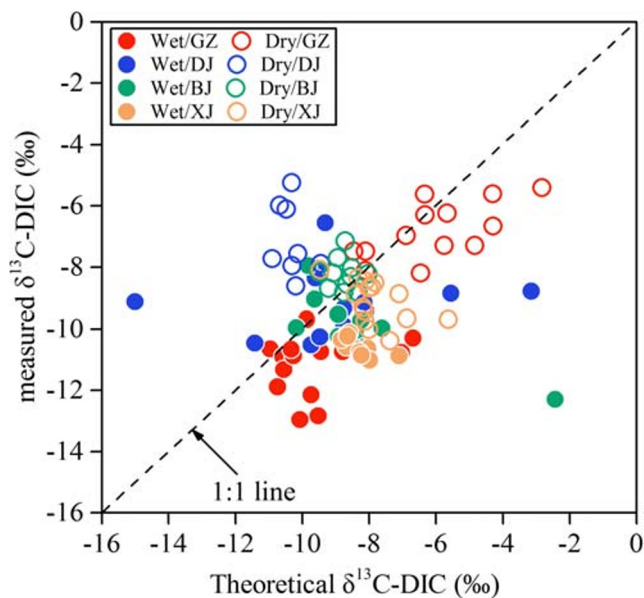


Fig. 8 Relationships of measured and theoretical $\delta^{13}\text{C-DIC}$ values of river water in the Pearl River Delta. The 1:1 line indicated measured $\delta^{13}\text{C-DIC}$ and theoretical $\delta^{13}\text{C-DIC}$ values were equal

proportion of DIC sources, and the increase in the proportion of DIC from carbonate dissolution by sulfuric and nitric acids would ultimately become a source of CO_2 to the atmosphere on the geological timescale and affect the CO_2 budget (Li et al. 2008). Figure 7b illustrates that most of the samples were located in the area defined by the three end-members, indicating that carbonate dissolution and silicate dissolution by carbonic, sulfuric, and nitric acids involved chemical weathering and had effects on ionic composition and carbon isotopes in river waters. To verify whether only these three end-members were the major contributors affecting the DIC in the river water, the theoretical $\delta^{13}\text{C-DIC}$ value was calculated based on the results of the contributions of different end-members in “Contribution of human activities to DIC” and the $\delta^{13}\text{C-DIC}$ signatures of each end-member. The calculated equation as follows:

$$\delta^{13}\text{C-DIC}_{\text{theoretical}} = (f1 \times -17\text{‰}) + (f2 \times -8.25\text{‰}) + (f3 \times +0.5\text{‰}) \quad (25)$$

The calculated results of the theoretical $\delta^{13}\text{C-DIC}$ values of river water are shown in Fig. 8. The differences between the measured and theoretical $\delta^{13}\text{C-DIC}$ values of most samples were within $\pm 2\text{‰}$, indicating that the $\delta^{13}\text{C-DIC}$ values of river waters were mainly controlled by the three isotopic end-members. Thus, the carbon isotopic signatures of DIC could be a useful tool to identify the sources and the $\delta^{13}\text{C-DIC}$ fingerprint could reflect the mixing effect of weathering processes in the river ecosystem (Ali and Atekwana 2011;

Jiang 2013). However, the differences between the measured and theoretical $\delta^{13}\text{C-DIC}$ values of some samples were large, suggesting that there might be other processes affecting the $\delta^{13}\text{C-DIC}$ value of river waters that are not accounted for by the isotopic end-members (Spence and Telmer 2005).

Biochemical alternation of the DIC pool River water chemistry is largely a production of chemical rock weathering, dissolution/hydrolysis, and mineral precipitation (Schulte et al. 2011). As discussed above, the three weathering processes were primarily responsible for the compositions of the $\delta^{13}\text{C-DIC}$. Biochemical processes, such as outgassing of CO_2 from the water-air interface (Spence and Telmer 2005; Varekamp et al. 2016), photosynthesis by phytoplankton (Liu et al. 2010; Wachniew 2006), and decomposition of organic matter by micro- and macro-organisms (de Medeiros Engelmann et al. 2018; Pozzato et al. 2018), are other controls of the enrichment or depletion of $\delta^{13}\text{C-DIC}$ values. In this study, (1) during the wet season, the measured $\delta^{13}\text{C-DIC}$ values were generally lower than the theoretical values (right of the 1:1 line in Fig. 8). This depleted $\delta^{13}\text{C-DIC}$ might be caused by increased respiration of organic matter due to high temperatures in the wet season (Barnes and Raymond 2009). (2) During the dry season, the measured $\delta^{13}\text{C-DIC}$ values were significantly higher than the theoretical values in the DJ River (left of the 1:1 line in Fig. 8), which might be associated with photosynthesis in the river water. Phytoplankton preferentially incorporate light ^{12}C over heavy ^{13}C during DIC uptake, leaving heavier $\delta^{13}\text{C}$ in the residual DIC (Hama et al. 1983; Rau et al. 2001). In addition, the increase in $\delta^{13}\text{C-DIC}$ during the dry season reflected the anthropogenic impact on the DIC pool. During the dry season, the nitrogen source in the river was mainly derived from a point source (e.g. sewage), coupled with an increase in nutrient concentration due to decreased precipitation and reduced runoff and flow velocity, which was beneficial to the growth of phytoplankton and subsequently increased the $\delta^{13}\text{C-DIC}$ signature. Moreover, in the dry season, the measured $\delta^{13}\text{C-DIC}$ values in the GZ Channel and DJ River were significantly higher than those in the BJ River and XJ River ($p < 0.01$), which further indicated that increased sewage discharge due to high degree of urbanization caused an enrichment of $\delta^{13}\text{C-DIC}$ (Barnes and Raymond 2009).

Overall, the evidence from both the chemical data and $\delta^{13}\text{C-DIC}$ of river water indicated that chemical compositions in the river water were controlled by both natural and anthropogenic factors in the PRD region, and carbonate dissolution by sulfuric and nitric acids introduced by human activities should be responsible for the increased $\delta^{13}\text{C-DIC}$ of river water. In addition, the $\delta^{13}\text{C-DIC}$ of river water was also affected by biogeochemical processes (e.g. photosynthesis and nitrification) due to isotope fractionation, and high $\delta^{13}\text{C-DIC}$ values in the highly urbanized area reflected anthropogenic

impacts on the $\delta^{13}\text{C}$ -DIC signatures. Therefore, human activities promoted the use of DIC by phytoplankton, thereby fixing carbon and decreasing the DIC flux, and the DIC contributed from carbonate dissolution by sulfuric and nitric acids caused by human activities would become a source of atmospheric CO_2 on the geological timescale.

Conclusions

The hydrochemical compositions and isotopic signatures of the dissolved inorganic carbon in the PRD region revealed that carbonate dissolution, silicate dissolution, and anthropogenic inputs provided the majority of the solutes in the river water. For the river water samples in the BJ River and XJ River, Ca^{2+} was the most abundant cation, accounting for 69% of the total cations, and HCO_3^- was the dominant anion, accounting for 75% of the total anions, which suggested that the chemical compositions were mainly contributed by carbonate dissolution. For the river water samples in the GZ Channel and DJ River, the proportions of Na^+ , Cl^- , SO_4^{2-} , and NO_3^- significantly increased, indicating that the increase in anthropogenic inputs contributed to the solutes in the river water. The results of principal component analysis showed that anthropogenic pollution and rock weathering were recognized as the main factors controlling the regional hydrochemistry. These two factor scores indicated the spatial variation in hydrochemistry. The water samples in the GZ Channel were characterized by high relative anthropogenic pollution factor; however, the influence of the rock weathering factor was greater in the XJ River and BJ River. In addition, significant seasonal variation in the DIC sources or relative biogeochemical processes of DIC were found by the evidence of $\delta^{13}\text{C}$ -DIC signatures.

As the major product of chemical weathering, DIC concentrations and their carbon isotopes provide a better understanding of the processes controlling regional hydrochemistry. The proportions of the contribution from three theoretical weathering processes to the DIC showed that the contributions of carbonate dissolution by carbonic acid to the total concentrations of DIC in river water were high in the BJ River and XJ River, and the contributions of silicate dissolution by carbonic acid were high in the GZ Channel and DJ River, which were related to different rock outcrops. The contributions of carbonate dissolution by sulfuric and nitric acids to the DIC were high in the GZ Channel and DJ River, which was associated with a higher degree of urbanization, indicating that human activities played important roles in chemical compositions in the river water. However, carbonate dissolution by sulfuric and nitric acids caused by human activities did not result in an increase of in the DIC flux but changed the distribution of DIC sources, and this part of DIC would ultimately become a source of CO_2 to the atmosphere on the geological timescale

and affect the CO_2 budget. The evidence of the $\delta^{13}\text{C}$ -DIC signature also indicated that human activities promoted photosynthesis of phytoplankton which changed the DIC pool.

Funding information This research work was financially supported by the Fundamental Research Funds for the Central Universities (Grant No.19lgpy148), the General Program of the National Natural Science Foundation of China (Grant No.41877470), and the National Key R&D Program of China (Nos. 2017YFB0903700 and 2017YFB0903703).

References

- Abdi H, Williams LJ (2010) Principal component analysis. Wiley Interdiscip Rev Comput Stat 2:433–459
- Ali HN, Atekwana EA (2011) The effect of sulfuric acid neutralization on carbonate and stable carbon isotope evolution of shallow groundwater. Chem Geol 284:217–228
- Assayag N, Rivé K, Ader M, Jézéquel D, Agrinier P (2006) Improved method for isotopic and quantitative analysis of dissolved inorganic carbon in natural water samples. Rapid Commun Mass Spectrom 20:2243–2251
- Barnes RT, Raymond PA (2009) The contribution of agricultural and urban activities to inorganic carbon fluxes within temperate watersheds. Chem Geol 266:318–327
- Berner RA, Kothavala Z (2001) GEOCARB III: a revised model of atmospheric CO_2 over Phanerozoic time. Am J Sci 301:182–204
- Brunet F et al (2005) $\delta^{13}\text{C}$ tracing of dissolved inorganic carbon sources in Patagonian rivers (Argentina). Hydrol Process 19:3321–3344
- Calmels D, Gaillardet J, François L (2014) Sensitivity of carbonate weathering to soil CO_2 production by biological activity along a temperate climate transect. Chem Geol 390:74–86
- Cao Y, Tang C, Cao G, Wang X (2016a) Hydrochemical zoning: natural and anthropogenic origins of the major elements in the surface water of Taizi River Basin, Northeast China. Environ Earth Sci 75:811
- Cao Y, Tang C, Song X, Liu C, Zhang Y (2016b) Identifying the hydrochemical characteristics of rivers and groundwater by multivariate statistical analysis in the Sanjiang Plain, China. Appl Water Sci 6:169–178
- Cartwright I (2010) The origins and behaviour of carbon in a major semi-arid river, the Murray River, Australia, as constrained by carbon isotopes and hydrochemistry. Appl Geochem 25:1734–1745
- Clark ID, Fritz P (2013) Environmental isotopes in hydrogeology. CRC Press, Boca Raton
- Cuomo E et al (2017) Geolithological and anthropogenic controls on the hydrochemistry of the Volturno river (Southern Italy). Hydrol Process 31
- de Medeiros Engelmann P, Dos Santos VHJM, Barbieri CB, Augustin AH, Ketzner JMM, Rodrigues LF (2018) Environmental monitoring of a landfill area through the application of carbon stable isotopes, chemical parameters and multivariate analysis. Waste Manag 76: 591–605
- Ding H et al (2017) Geochemistry of the dissolved loads of the Liao River basin in northeast China under anthropogenic pressure: chemical weathering and controlling factors. J Asian Earth Sci 138:657–671
- Du S, Van Rompaey A, Shi P, Wang Ja (2015) A dual effect of urban expansion on flood risk in the Pearl River Delta (China) revealed by land-use scenarios and direct runoff simulation. Nat Hazards 77: 111–128
- Dubois KD, Lee D, Veizer J (2010) Isotopic constraints on alkalinity, dissolved organic carbon, and atmospheric carbon dioxide fluxes in the Mississippi River. J Geophys Res Biogeosci:115
- Faure G (1977) Principles of Isotope Geology. Wiley, New York 589

- Gandois L, Perrin A-S, Probst A (2011) Impact of nitrogenous fertiliser-induced proton release on cultivated soils with contrasting carbonate contents: a column experiment. *Geochim Cosmochim Acta* 75:1185–1198
- Gao Q, Wang Z (2015) Dissolved inorganic carbon in the Xijiang River: concentration and stable isotopic composition. *Environ Earth Sci* 73:253–266
- Gao Q et al (2009) Chemical weathering and CO₂ consumption in the Xijiang River basin, South China. *Geomorphology* 106:324–332
- Guo J, Wang F, Vogt RD, Zhang Y, Liu CQ (2015) Anthropogenically enhanced chemical weathering and carbon evasion in the Yangtze Basin. *Sci Rep* 5:11941
- Halas S, Szaran J, Niezgoda H (1997) Experimental determination of carbon isotope equilibrium fractionation between dissolved carbonate and carbon dioxide. *Geochim Cosmochim Acta* 61:2691–2695
- Hama T et al (1983) Measurement of photosynthetic production of a marine phytoplankton population using a stable ¹³C isotope. *Mar Biol* 73(1):31–36
- Hartmann J, Moosdorf N, Lauerwald R, Hinderer M, West AJ (2014) Global chemical weathering and associated P-release—the role of lithology, temperature and soil properties. *Chem Geol* 363:145–163
- Hu J, Li S (2009) Modeling the mass fluxes and transformations of nutrients in the Pearl River Delta, China. *J Mar Syst* 78:146–167
- Jiang Y (2013) The contribution of human activities to dissolved inorganic carbon fluxes in a karst underground river system: evidence from major elements and $\delta^{13}\text{C}_{\text{DIC}}$ in Nandong, Southwest China. *J Contam Hydrol* 152:1–11
- Lerman A, Wu L (2006) CO₂ and sulfuric acid controls of weathering and river water composition. *J Geochem Explor* 88:427–430
- Levin I, Graul R, Trivett NBA (1995) Long-term observations of atmospheric CO₂ and carbon isotopes at continental sites in Germany. *Tellus B* 47:23–34
- Li S-L, Calmels D, Han G, Gaillardet J, Liu C-Q (2008) Sulfuric acid as an agent of carbonate weathering constrained by $\delta^{13}\text{C}_{\text{DIC}}$: examples from Southwest China. *Earth Planet Sci Lett* 270:189–199
- Li X et al (2019) Hydrochemistry and dissolved inorganic carbon (DIC) cycling in a tropical agricultural river, Mun River Basin, Northeast Thailand. *Int J Environ Res Public Health* 16:3410
- Liu Z, Dreybrodt W, Wang H (2010) A new direction in effective accounting for the atmospheric CO₂ budget: considering the combined action of carbonate dissolution, the global water cycle and photosynthetic uptake of DIC by aquatic organisms. *Earth Sci Rev* 99:162–172
- Liu W et al (2018a) Geochemistry of the dissolved loads during high-flow season of rivers in the southeastern coastal region of China: anthropogenic impact on chemical weathering and carbon sequestration. *Biogeosciences* 15:1726–1740
- Liu X et al (2018b) High-resolution multi-temporal mapping of global urban land using Landsat images based on the Google Earth Engine Platform. *Remote Sens Environ* 209:227–239
- Lu F-H, Ni H-G, Liu F, Zeng EY (2009) Occurrence of nutrients in riverine runoff of the Pearl River Delta, South China. *J Hydrol* 376:107–115
- Michel M (2003) Global analysis of river systems: from Earth system controls to Anthropocene syndromes. *Philos Trans Biol Sci* 358:1935–1955
- Murphy BP, Johnson JPL, Gasparini NM, Sklar LS (2016) Chemical weathering as a mechanism for the climatic control of bedrock river incision. *Nature* 532:223–227
- Niinikoski PIA, Karhu JA (2017) Natural vs. anthropogenic effects in the composition of dissolved inorganic carbon in a boreal river with a seasonal base flow component. *Hydrol Res* 48:1585–1593
- Ou S et al (2019) The influence of runoff and wind on the dispersion patterns of suspended sediment in the Zhujiang (Pearl) River Estuary based on MODIS data. *Acta Oceanol Sin* 38:26–35
- Peter AR, James EB (2000) Bacterial consumption of DOC during transport through a temperate estuary. *Aquat Microb Ecol* 22:1–12
- Pozzato L et al (2018) Origin of remineralized organic matter in sediments from the Rhone River prodelta (NW Mediterranean) traced by $\Delta^{14}\text{C}$ and $\delta^{13}\text{C}$ signatures of pore water DIC. *Prog Oceanogr* 163:0079–6611
- Rasse DP et al (2001) Modelling short-term CO₂ fluxes and long-term tree growth in temperate forests with ASPECTS. *Ecol Model* 141:35–52
- Rau GH, Chavez FP, Friederich GE (2001) Plankton ¹³C/¹²C variations in Monterey Bay, California: evidence of non-diffusive inorganic carbon uptake by phytoplankton in an upwelling environment. *Deep-Sea Res I Oceanogr Res Pap* 48:79–94
- Raymond PA, Oh N-H, Turner RE, Broussard W (2008) Anthropogenically enhanced fluxes of water and carbon from the Mississippi River. *Nature* 451:449
- Samanta S, Dalai TK, Pattanaik JK, Rai SK, Mazumdar A (2015) Dissolved inorganic carbon (DIC) and its $\delta^{13}\text{C}$ in the Ganga (Hooghly) River estuary, India: evidence of DIC generation via organic carbon degradation and carbonate dissolution. *Geochim Cosmochim Acta* 165:226–248
- Schulte P et al (2011) Applications of stable water and carbon isotopes in watershed research: weathering, carbon cycling, and water balances. *Earth Sci Rev* 109:20–31
- Spence J, Telmer K (2005) The role of sulfur in chemical weathering and atmospheric CO₂ fluxes: evidence from major ions, $\delta^{13}\text{C}_{\text{DIC}}$, and $\delta^{34}\text{S}_{\text{SO}_4}$ in rivers of the Canadian Cordillera. *Geochim Cosmochim Acta* 69:5441–5458
- Strokal M et al (2015) Increasing dissolved nitrogen and phosphorus export by the Pearl River (Zhujiang): a modeling approach at the sub-basin scale to assess effective nutrient management. *Biogeochemistry* 125:221–242
- Telmer K, Veizer J (1999) Carbon fluxes, pCO₂ and substrate weathering in a large northern river basin, Canada: carbon isotope perspectives. *Chem Geol* 159:61–86
- Varekamp JC, Caldwell S, Capece L, Horne J, Upin H (2016) The Newberry crater lakes, Oregon. *Keck Geology Consortium, 29th Annual Symposium Volume*
- Veizer J et al (1999) ⁸⁷Sr/⁸⁶Sr, $\delta^{13}\text{C}$ and $\delta^{18}\text{O}$ evolution of Phanerozoic seawater. *Chem Geol* 161:59–88
- Vogel JC (1993) Variability of carbon isotope fractionation during photosynthesis. In: *Stable Isotopes and Plant Carbon-Water Relations*. Academic, San Diego, pp 29–38
- Wachniew P (2006) Isotopic composition of dissolved inorganic carbon in a large polluted river: the Vistula, Poland. *Chem Geol* 233:293–308
- Wen J, Tang C, Cao Y, Li X, Chen Q (2018) Hydrochemical evolution of groundwater in a riparian zone affected by acid mine drainage (AMD), South China: the role of river–groundwater interactions and groundwater residence time. *Environ Earth Sci* 77:794
- Xia D et al (2017) Isotope geochemistry, hydrochemistry, and mineralogy of a river affected by acid mine drainage in a mining area, South China. *RSC Adv* 7:43310–43318
- Xie GQ, Zhen T, Longhai L, Lishanchi (2013) Chemical weathering and CO₂ consumption in the Dongjiang River Basin. *Acta Sci Circumst* 33:2123–2133
- Xu Q et al (2019) Temporal and spatial differences in carbon emissions in the Pearl River Delta based on multi-resolution emission inventory modeling. *J Clean Prod* 214:615–622
- Xuan Y et al (2018) Spatial and temporal variation of hydro-chemistry and chemical weathering characteristics in the Beiji River Basin. [in Chinese with English abstract]. *Res Environ Sci* 31:1078–1087
- Yang M, Liu Z, Sun H, Yang R, Chen B (2016) Organic carbon source tracing and DIC fertilization effect in the Pearl River: insights from lipid biomarker and geochemical analysis. *Appl Geochem* 73:132–141

- Ye F, Jia G, Xie L, Wei G, Xu J (2016) Isotope constraints on seasonal dynamics of dissolved and particulate N in the Pearl River Estuary, south China. *J Geophys Res* 121:8689–8705
- Ye F, Guo W, Shi Z, Jia G, Wei G (2017) Seasonal dynamics of particulate organic matter and its response to flooding in the Pearl River Estuary, China, revealed by stable isotope ($\delta^{13}\text{C}$ and $\delta^{15}\text{N}$) analyses. *J Geophys Res Oceans* 122:6835–6856
- Yidana SM, Ophori D, Banoeng-Yakubo B (2008) A multivariate statistical analysis of surface water chemistry data—the Ankobra Basin, Ghana. *J Environ Manag* 86:80–87
- Yu F et al (2010) Bulk organic $\delta^{13}\text{C}$ and C/N as indicators for sediment sources in the Pearl River delta and estuary, southern China. *Estuar Coast Shelf Sci* 87:618–630
- Yu H et al (2015) Seasonal variations in the nitrogen isotopic composition of dissolved nitrate in the Changjiang River estuary, China. *Estuar Coast Shelf Sci* 155:148–155
- Zavadlav S, Kanduč T, McIntosh J, Lojen S (2013) Isotopic and chemical constraints on the biogeochemistry of dissolved inorganic carbon and chemical weathering in the karst watershed of Krka River (Slovenia). *Aquat Geochem* 19:209–230
- Zeng C, Liu Z, Zhao M, Yang R (2016) Hydrologically-driven variations in the karst-related carbon sink fluxes: insights from high-resolution monitoring of three karst catchments in Southwest China. *J Hydrol* 533:74–90
- Zhang J, Quay PD, Wilbur DO (1995) Carbon isotope fractionation during gas-water exchange and dissolution of CO_2 . *Geochim Cosmochim Acta* 59:107–114
- Zhang SR et al (2007) Water chemistry of the Zhujiang (Pearl River): natural processes and anthropogenic influences. *J Geophys Res J Geophys Res Atmos* 112:137–161
- Zhou H, Shi P, Wang Ja, Yu D, Gao L (2011) Rapid urbanization and implications for river ecological services restoration: case study in Shenzhen, China. *J Urban Plann Dev* 137:121–132

Publisher's note Springer Nature remains neutral with regard to jurisdictional claims in published maps and institutional affiliations.